

The Snell's laws at interfaces in anisotropic viscoelastic media

Václav Vavryčuk

*Institute of Geophysics, Academy of Sciences, Boční II/1401, Praha 4, Czech Republic,
vv@ig.cas.cz*

SUMMARY

The behaviour of rays at interfaces in anisotropic viscoelastic media is studied using three different approaches: the real elastic ray theory, the real viscoelastic ray theory and the complex ray theory. In solving the complex eikonal equation, the highest accuracy is achieved by the complex ray theory. The real elastic and viscoelastic ray theories are less accurate but computationally more effective. In all three approaches, the rays obey Snell's law at the interface, but its form is different for each approach. The complex Snell's law constrains the complex tangential components of the slowness vector. The real viscoelastic and elastic Snell's laws constrain the real tangential components of the slowness vector. In the viscoelastic ray theory, besides Snell's law, the condition of stationary slowness vector is imposed in calculating the rays of scattered waves. The accuracy of all three ray theoretical approaches is numerically tested by solving the complex eikonal equation. The models of the medium consist of attenuating isotropic and anisotropic homogeneous halfspaces. The level of attenuation ranges from extremely strong ($Q = 2.5-3$) to moderate attenuation ($Q = 25-30$). Numerical modelling shows that the real viscoelastic ray approach is highly accurate being at least 20 times more accurate than the real elastic ray approach.

Keywords: anisotropy, attenuation, complex eikonal equation, ray theory, seismic waves, wave propagation

1. INTRODUCTION

Applications of the ray theory to wave propagation problems in anisotropic, inhomogeneous and attenuating media have been intensively studied in recent years (Thomson 1997; Hanyga & Seredyńska 2000; Carcione 2006; Vavryčuk 2007a,b; Červený *et al.* 2008; Vavryčuk 2008a,b). The ray theory yields a high-frequency approximation

which is reasonably accurate in most seismic applications (Červený 2001), and computationally undemanding with respect to other methods solving the equation of motion numerically (Carcione 1990, 1993; Saenger & Bohlen 2004; Moczo *et al.* 2004, 2007). So far, several ray-theoretical approaches for solving the eikonal equation and modelling of waves in anisotropic attenuating media have been developed. The simplest approach is constructing the rays and other ray quantities in the elastic reference medium and incorporating the effects of attenuation as perturbations (Gajewski & Pšenčík 1992; Vavryčuk 2008b). However, this procedure is applicable to weakly attenuating media only. Alternatively, several authors tried to develop the theory of complex rays (Hearn & Krebes 1990a,b; Le *et al.* 1994; Thomson 1997; Chapman *et al.* 1999; Kravtsov *et al.* 1999; Hanyga & Seredyńska 2000; Kravtsov 2005; Amodei *et al.* 2006). The attenuation is incorporated into the wave modelling by substituting the real-valued elastic parameters by complex-valued and frequency-dependent viscoelastic parameters. Consequently, the eikonal equation and other ray equations become complex and their solution is sought in complex space. The complex ray theory is very accurate in solving the complex eikonal equation, and applicable to anisotropy and attenuation of arbitrary strength. Unfortunately, this theory is computationally complicated and conditioned by successful building of the velocity model in complex space.

Another ray-theoretical approach applicable to solving the complex eikonal equation has been proposed by Vavryčuk (2008a) and called the real viscoelastic ray method. It produces real rays, but all quantities along the rays are complex-valued. The approach is based on the assumption that the complex slowness vector along a ray is stationary and the complex energy velocity vector is homogenous. The viscoelastic ray approach is less accurate than the complex ray approach, but has proved to be efficient and significantly more accurate than the elastic ray approach (Vavryčuk 2009).

So far, the viscoelastic ray theory has been developed and all numerical tests have been performed in smoothly inhomogeneous media. In this paper, the theory is completed by deriving formulas for the behaviour of rays at interfaces in anisotropic attenuating media. It is shown that the rays of scattered waves must obey Snell's law, which is similar but not identical with Snell's law in elastic media. The derived theoretical formulas are numerically tested by solving the complex eikonal equation in models of isotropic and anisotropic homogeneous halfspaces with various levels of attenuation. The accuracy of the viscoelastic ray tracing is compared with that produced by real elastic ray tracing and complex ray tracing.

2. ANISOTROPIC VISCOELASTIC MEDIUM

2.1. Notation

In formulas, the real and imaginary parts of the complex-valued quantities are denoted by superscripts R and I , respectively. A complex-conjugate quantity is denoted by an asterisk. The direction of a complex-valued vector \mathbf{v} is calculated as $\mathbf{v}/\sqrt{\mathbf{v}^T \mathbf{v}}$, where the superscript T means transposition. The magnitude of complex-valued vector \mathbf{v} is complex and is calculated as $\sqrt{\mathbf{v}^T \mathbf{v}}$. If any complex-valued vector is defined by a real-valued direction, it is called homogeneous, and if defined by a complex-valued direction, it is called inhomogeneous.

Besides the standard four-index notation for viscoelastic parameters a_{ijkl} and quality parameters q_{ijkl} , also the two-index Voigt notation A_{MN} and Q_{MN} is used alternatively. The Voigt notation combines pairs of indices i,j or k,l into a single index M or N using the following rules:

$$11 \rightarrow 1, 22 \rightarrow 2, 33 \rightarrow 3, 23 \rightarrow 4, 13 \rightarrow 5, \text{ and } 12 \rightarrow 6. \quad (1)$$

Quantities in the frequency domain are calculated using the Fourier transform defined as follows:

$$f(\omega) = F[f(t)] = \int_{-\infty}^{\infty} f(t) \exp(i\omega t) dt. \quad (2)$$

In formulas, the Einstein summation convention is used for repeated subscripts.

2.2 Viscoelastic parameters

A viscoelastic medium is defined by density-normalized viscoelastic parameters a_{ijkl} which are, in general, complex-valued, frequency-dependent and vary with position vector \mathbf{x} . The real and imaginary parts of a_{ijkl} ,

$$a_{ijkl}(\mathbf{x}, \omega) = a_{ijkl}^R + i a_{ijkl}^I, \quad (3)$$

define elastic and viscous properties of the medium. The ratio between the real and imaginary parts of a_{ijkl} is called the matrix of quality factor parameters,

$$q_{ijkl}(\mathbf{x}, \omega) = -\frac{a_{ijkl}^R}{a_{ijkl}^I} \quad (\text{no summation over repeated indices}), \quad (4)$$

and quantifies how attenuating the medium is. The sign in eq. (4) depends on the definition of the Fourier transform (2) used for calculating the viscoelastic parameters in the frequency domain. When using the Fourier transform with the exponential term $\exp(-i\omega t)$, the minus sign in (4) must be omitted.

2.3 Complex eikonal equation

The equation of motion for an inhomogeneous anisotropic viscoelastic medium, when no sources are considered, reads (see Červený, 2001, Eq. 2.1.27),

$$\rho \omega^2 u_i + (\rho a_{ijkl} u_{k,l})_{,j} = 0, \quad i = 1,2,3, \quad (5)$$

where $\mathbf{u} = \mathbf{u}(\mathbf{x}, \omega)$ is the displacement, $\rho = \rho(\mathbf{x})$ is the density of the medium, $a_{ijkl} = a_{ijkl}(\mathbf{x}, \omega)$ are the density-normalized viscoelastic parameters, and ω is the circular frequency. Frequency ω , density ρ , and position vector \mathbf{x} are real-valued, viscoelastic parameters a_{ijkl} and displacement \mathbf{u} are complex-valued. Displacement $\mathbf{u} = \mathbf{u}(\mathbf{x}, \omega)$ is assumed to describe a high-frequency harmonic signal,

$$u_i(\mathbf{x}, \omega) = U_i(\mathbf{x}) \exp[i\omega\tau(\mathbf{x})], \quad (6)$$

where $\mathbf{U} = \mathbf{U}(\mathbf{x})$ is the complex-valued amplitude, and $\tau = \tau(\mathbf{x})$ is the complex-valued travel time. Inserting eq. (6) into the equation of motion (5), we obtain the eikonal equation in the form

$$G(\mathbf{x}, \mathbf{p}) = a_{ijkl} p_i p_l g_j g_k = 1, \quad (7)$$

where G is the eigenvalue and \mathbf{g} is the normalized complex-valued eigenvector, $\mathbf{g} \cdot \mathbf{g} = 1$, of the Christoffel tensor of the studied wave (P , $S1$ or $S2$)

$$\Gamma_{jk}(\mathbf{x}, \mathbf{p}) = a_{ijkl} p_i p_l, \quad (8)$$

and vector \mathbf{p} is the complex-valued slowness vector defined as

$$p_i = \frac{\partial \tau}{\partial x_i}. \quad (9)$$

3. REAL VISCOELASTIC RAY TRACING IN SMOOTHLY INHOMOGENEOUS MEDIA

3.1. Anisotropic media

The eikonal equation (7) can alternatively be expressed in the following general form (see Červený, 2001, Eq. 3.6.3)

$$H(\mathbf{x}, \mathbf{p}) = \frac{1}{2}(G(\mathbf{x}, \mathbf{p}) - 1) = 0, \quad (10)$$

where $H = H(\mathbf{x}, \mathbf{p})$ is the Hamiltonian. The eikonal equation in the Hamiltonian form (10) represents a non-linear partial differential equation for the complex travel time $\tau = \tau(\mathbf{x})$. This equation can be solved exactly by using the complex ray-tracing equations with complex-valued generalized coordinates \mathbf{x} and \mathbf{p} (see Section 5.1). It can also be solved approximately using the real viscoelastic ray-tracing equations with real-valued generalized coordinates \mathbf{x} and \mathbf{p}^R (see Vavryčuk 2008a), where

$$p_i^R = \frac{\partial \tau^R}{\partial x_i}. \quad (11)$$

The inverse quantity to \mathbf{p}^R is the ray velocity \mathbf{V}^{ray} ,

$$V_i^{\text{ray}} = \frac{dx_i}{d\tau^R}, \quad (12)$$

which physically means the velocity of a signal propagating along a ray. Equations (11) and (12) imply the following identity:

$$V_j^{\text{ray}} p_j^R = 1. \quad (13)$$

The real viscoelastic ray-tracing equations read

$$\frac{dx_i}{d\tau^R} = \frac{1}{2} \frac{\partial G}{\partial p_i^R}, \quad \frac{dp_i^R}{d\tau^R} = -\frac{1}{2} \frac{\partial G}{\partial x_i}. \quad (14)$$

Substituting (7) into (14) we obtain (see Vavryčuk 2008a, eqs 29, 35 and A7)

$$\frac{dx_i}{d\tau^R} = N_i \frac{v^R v^R + v^I v^I}{v^R}, \quad (15)$$

$$\frac{dp_i^R}{d\tau^R} = -\frac{1}{2} \left[\left(\frac{\partial a_{jklm}}{\partial x_i} p_j p_m g_k g_l \right)^R + \frac{v^I}{v^R} \left(\frac{\partial a_{jklm}}{\partial x_i} p_j p_m g_k g_l \right)^I \right], \quad (16)$$

$$\frac{d\tau^I}{d\tau^R} = -\frac{v^I}{v^R}, \quad (17)$$

where energy velocity vector \mathbf{v} ,

$$v_i = a_{ijkl} p_l g_j g_k, \quad (18)$$

is a complex homogeneous vector. This means that the real and imaginary parts of the energy velocity vector are parallel. This condition restricts possible values of the complex slowness vector and implies that the real and imaginary parts of the slowness vector in the ray-tracing equations are not independent. The slowness vector, which predicts a homogeneous energy velocity vector, is called *stationary* (see Vavryčuk 2007a,b). The stationary slowness vector is, in general, inhomogeneous. The procedure, how to calculate the stationary slowness vector \mathbf{p} is described in Vavryčuk (2008a).

3.2. Isotropic media

The eigenvalue of the Christoffel tensor G in isotropic media reads

$$G(\mathbf{x}, \mathbf{p}^R) = c^2 p_i p_i = 1, \quad (19)$$

where c is the complex-valued phase velocity, $c = \sqrt{(\lambda + 2\mu)/\rho}$ for the P wave, and $c = \sqrt{\mu/\rho}$ for the S wave. Parameters λ and μ are complex-valued Lamé's coefficients.

Vector \mathbf{p} is the complex-valued slowness vector, $p_i = \frac{\partial \tau}{\partial x_i}$, its magnitude is $p = 1/c$,

vector \mathbf{p}^R is its real-valued part, $p_i^R = \frac{\partial \tau^R}{\partial x_i}$, and τ is the complex-valued travel time. Since

the energy velocity vector \mathbf{v} ,

$$v_i = c^2 p_i. \quad (20)$$

is homogeneous, slowness vector \mathbf{p} must also be homogeneous. This simplifies the ray-tracing problem, and the ray-tracing equations in anisotropic media (15)-(17) are reduced to the following form in isotropic media (see Vavryčuk 2008a, eqs 39 and A7)

$$\frac{dx_i}{d\tau^R} = V^2 p_i^R, \quad \frac{dp_i^R}{d\tau^R} = -\frac{1}{V} \frac{\partial V}{\partial x_i}, \quad \frac{d\tau^I}{d\tau^R} = -\frac{c^I}{c^R} \quad (21)$$

where V is the real-valued phase velocity calculated from the complex-valued phase velocity c as,

$$V = \frac{1}{(c^{-1})^R}, \quad (22)$$

and τ^R is the real part of travel time τ . Obviously, $V^{\text{ray}} = V$ and $p^R = 1/V^{\text{ray}}$.

4. REAL VISCOELASTIC RAYS AT INTERFACES

4.1. Viscoelastic Snell's law in anisotropic media

Let us assume two homogeneous halfspaces separated by a smoothly curved interface with normal \mathbf{n} . This medium can be viewed as a limiting case of a smoothly inhomogeneous medium with a thin transition layer displaying a strong gradient, and the width of the layer shrinking to zero. In this way, we can utilize the ray-tracing equations to derive Snell's law. Accordingly, we immediately see that the second ray-tracing equation in (14) implies that the tangential component of vector \mathbf{p}^R is conserved across the interface:

$$\mathbf{p}_\Sigma^R = \mathbf{p}^R - \mathbf{n}(\mathbf{p}^R \cdot \mathbf{n}) = \text{const}. \quad (23)$$

Since generally three waves are reflected and three waves are transmitted at the interface in anisotropic viscoelastic media, we can express Snell's law in the following form:

$$\mathbf{p}_\Sigma^{(W)R} = \mathbf{p}_\Sigma^{(0)R}, \quad (24)$$

where superscript 0 denotes the incident wave, and superscript $W = 1, \dots, 6$, denotes the type of scattered wave (P , $S1$ and $S2$ reflected, and P , $S1$ and $S2$ transmitted). Equation (24) is the real viscoelastic Snell's law. It is emphasized that Snell's law constrains only the real

parts of slowness vectors \mathbf{p}^R , but not the complete complex-valued slowness vectors \mathbf{p} . For elastic media, eq. (24) transforms to the elastic Snell's law.

4.2. Slowness vectors \mathbf{p} of scattered waves

The real viscoelastic Snell's law prescribes the value of the tangential component of \mathbf{p}^R at the interface for all scattered waves. The complete complex-valued slowness vector \mathbf{p} must satisfy two conditions. First, it must satisfy the Christoffel equation, and second, it must be stationary. Let us decompose vector \mathbf{p} into its normal and tangential components as follows:

$$\mathbf{p} = \sigma \mathbf{n} + \mathbf{p}_\Sigma = \sigma \mathbf{n} + \mathbf{p}_\Sigma^R + i \mathbf{p}_\Sigma^I, \quad (25)$$

where vector \mathbf{n} is the real-valued normal to interface Σ and σ is the complex-valued scalar. We have to find σ and \mathbf{p}_Σ^I for each scattered wave. If we assume that not only \mathbf{p}_Σ^R , but also \mathbf{p}_Σ^I is known, we can then calculate σ from the equation for the eigenvalue of the Christoffel tensor Γ_{jk} ,

$$\det(\Gamma_{jk} - \delta_{jk}) = 0, \quad (26)$$

which represents an algebraic equation of the 6th degree in σ . Alternatively, we can follow Červený & Pšenčík (2005) and find σ by solving the eigenvalue problem of the 6x6 complex-valued matrix $\mathbf{\Pi}$,

$$\det(\mathbf{\Pi} - \sigma \mathbf{I}_6) = 0, \quad (27)$$

where \mathbf{I}_m denotes the $m \times m$ identity matrix and matrix $\mathbf{\Pi}$ is expressed by four 3x3 submatrices,

$$\mathbf{\Pi} = \begin{bmatrix} \mathbf{\Pi}_{11} & \mathbf{\Pi}_{12} \\ \mathbf{\Pi}_{21} & \mathbf{\Pi}_{22} \end{bmatrix}, \quad (28)$$

which are defined as follows

$$\begin{aligned} \mathbf{\Pi}_{11} &= -[\mathbf{C}^{(1)}]^{-1} \mathbf{C}^{(2)} = \mathbf{\Pi}_{22}^T, & \mathbf{\Pi}_{12} &= -[\mathbf{C}^{(1)}]^{-1}, \\ \mathbf{\Pi}_{21} &= -\mathbf{I}_3 + \mathbf{C}^{(4)} - \mathbf{C}^{(3)} [\mathbf{C}^{(1)}]^{-1} \mathbf{C}^{(2)}, & \mathbf{\Pi}_{22} &= -\mathbf{C}^{(3)} [\mathbf{C}^{(1)}]^{-1}, \end{aligned} \quad (29)$$

with

$$C_{ik}^{(1)} = a_{ijkl} n_j n_l, \quad C_{ik}^{(2)} = a_{ijkl} n_j p_{\Sigma l}, \quad C_{ik}^{(3)} = a_{ijkl} p_{\Sigma j} n_l, \quad C_{ik}^{(4)} = a_{ijkl} p_{\Sigma j} p_{\Sigma l}. \quad (30)$$

Calculating σ , we can determine the complete slowness vector \mathbf{p} , and subsequently polarization vector \mathbf{g} , complex energy velocity vector \mathbf{v} , and finally the ray direction \mathbf{N} , $\mathbf{N} = \mathbf{v}/v$.

If vector \mathbf{p}'_{Σ} is chosen arbitrarily, the above procedure will yield a generally complex-valued ray direction \mathbf{N} . Since the stationary slowness vector must predict real-valued ray direction \mathbf{N} , the procedure must be inverted. The task for the inversion is to find two real-valued components of vector \mathbf{p}'_{Σ} which yield the real-valued ray direction \mathbf{N} . Since the magnitude of vector \mathbf{p}'_{Σ} is usually small, an inversion with iterations can be applied and several iterations lead to success in most cases.

4.3. Viscoelastic Snell's law in isotropic media

The real viscoelastic Snell's law in isotropic media has the same form as in anisotropic media (see eq. 24). However, calculating the complete slowness vectors \mathbf{p} of scattered waves is much simpler in isotropy than in anisotropy. Since the stationary slowness vector is homogeneous (see Section 3.2), vectors \mathbf{p}^R and \mathbf{p}^I are parallel,

$$\mathbf{p} = \mathbf{p}^R + i\mathbf{p}^I = (V^{-1} + iA)\mathbf{N} = V^{-1}(1 + iAV)\mathbf{N}, \quad (31)$$

where \mathbf{N} is the ray direction and A is the ray attenuation (see Vavryčuk 2007b)

$$A = (c^{-1})^I. \quad (32)$$

No inversion problem for calculating \mathbf{p}^I has to be solved. The normal component of vector \mathbf{p}^R is directly obtained as

$$\mathbf{p}_n^R = \pm \sqrt{V^{-2} - \mathbf{p}_{\Sigma}^R \cdot \mathbf{p}_{\Sigma}^R}, \quad (33)$$

and the normal and tangential components of \mathbf{p}^I read

$$\mathbf{p}_n^I = AV \mathbf{p}_n^R, \quad \mathbf{p}_{\Sigma}^I = AV \mathbf{p}_{\Sigma}^R. \quad (34)$$

The sign in eq. (33) is chosen in the same way as in elastic media. For subcritical incidences the sign discriminates between reflected and transmitted waves. For overcritical incidences, the slowness vector \mathbf{p} of transmitted wave becomes inhomogeneous and the sign of its imaginary normal component must be chosen to satisfy the radiation conditions.

5. ALTERNATIVE APPROACHES

5.1. Complex Snell's law

The most accurate method for solving the complex eikonal equation is the complex ray theory. In anisotropic smoothly inhomogeneous media, we apply the complex ray tracing equations,

$$\frac{dx_i}{d\tau} = a_{ijkl} p_l g_j g_k, \quad (35)$$

$$\frac{dp_i}{d\tau} = -\frac{1}{2} \frac{\partial a_{jkl}}{\partial x_i} p_k p_n g_j g_l, \quad (36)$$

where all quantities are complex-valued including the ray trajectory $\mathbf{x} = \mathbf{x}(\tau)$. Only the start and end points of the ray (i.e., the source and the receiver) lie in real space. This implies that viscoelastic stiffness parameters $a_{ijkl} = a_{ijkl}(\mathbf{x})$ usually considered as functions in real space, must be defined as functions in complex space. Parameters a_{ijkl} can be defined in complex space by analytical continuation of a_{ijkl} from the real to the complex space. However, this procedure is complicated and as yet applicable to simple models only (see Vavryčuk 2009, Appendix A).

At interfaces, we apply the continuity condition of the complex travel time and the complex Snell's law (Borcherdt R.D., 1977, 1982; Caviglia. & Morro, 1992; Wennerberg 1985; Winterstein 1987; Carcione 2007; Červený 2007)

$$\mathbf{p}_\Sigma^{(W)} = \mathbf{p}_\Sigma^{(0)}, \quad (37)$$

where superscript 0 denotes the incident wave and superscript $W = 1, \dots, 6$ denotes the type of scattered wave (P , $S1$ and $S2$ reflected, and P , $S1$ and $S2$ transmitted). It is emphasized that the complex Snell's law constrains the real as well as the imaginary part of the tangential component \mathbf{p}_Σ of the slowness vectors, but not just the real parts \mathbf{p}_Σ^R as assumed

in the real viscoelastic Snell's law. The normal components of \mathbf{p} of the scattered waves must be calculated at the interface using the Christoffel equation.

5.2. Elastic Snell's law

A simple approximate method of incorporating attenuation into the ray theory is tracing rays in the elastic reference medium and calculating the effects of attenuation using the first-order perturbations (Gajewski & Pšenčík 1992; Vavryčuk 2008b). The ray tracing equations are identical with those for the elastic reference medium (see Červený 2001, eq. 3.6.10),

$$\frac{dx_i^R}{d\tau^R} = a_{ijkl}^R p_l^R g_j^R g_k^R, \quad (38)$$

$$\frac{dp_i^R}{d\tau^R} = -\frac{1}{2} \frac{\partial a_{ijkl}^R}{\partial x_i^R} p_k^R p_n^R g_j^R g_l^R, \quad (39)$$

where all quantities are real-valued. The ray-tracing equations are supplemented by an additional equation for τ^I (see Gajewski & Pšenčík, 1992, eq. 10; Vavryčuk 2008b, eq. 59)

$$\frac{d\tau^I}{d\tau^R} = -\frac{1}{2} a_{ijkl}^I p_i^R p_l^R g_j^R g_k^R. \quad (40)$$

At interfaces, the elastic Snell's law reads,

$$\mathbf{p}_\Sigma^{(W)R} = \mathbf{p}_\Sigma^{(0)R}. \quad (41)$$

The imaginary parts of the slowness vectors \mathbf{p} are identically zero.

The elastic ray approach is approximate and works mostly for weakly attenuating media. Its accuracy can be enhanced by incorporating higher-order perturbations (Klimeš 2002). In several aspects, the elastic and viscoelastic ray approaches are similar. Both approaches solve \mathbf{x} , \mathbf{p}^R and τ^I as a function of τ^R and produce real rays. However, the computed ray fields and travel time $\tau = \tau(\mathbf{x})$ are not identical. The differences are more pronounced in media with strong attenuation. In media with weak attenuation, the differences between both approaches are of the order of the second and higher perturbations.

6. NUMERICAL EXAMPLES

6.1. Medium model

In this section, the efficiency of the approaches presented above is tested numerically. A point source situated in the medium consisting of two homogenous viscoelastic halfspaces is considered. The halfspaces are in welded contact. Two models are studied: Model A consisting of two isotropic halfspaces and Model B consisting of two transversely isotropic halfspaces with a vertical axis of symmetry. For both models, three levels of attenuation are considered, ranging from extremely strong attenuation with Q of 2.5-3.0 to moderate attenuation with Q of 25-30 (see Tabs 1 and 2). The models with the extremely strong attenuation are unrealistic and probably do not reflect any seismic structure. Here they are used to check the robustness of the developed ray methods.

Table 1: Viscoelastic parameters of Models A

Model	Upper halfspace		Lower halfspace	
	μ^R	Q	μ^R	Q
A1	1.0	5	0.5	2.5
A2	1.0	25	0.5	12.5
A3	1.0	50	0.5	25

Table 2: Viscoelastic parameters of Models B

Model	Upper halfspace				Lower halfspace			
	a_{44}^R	a_{66}^R	Q_{44}	Q_{66}	a_{44}^R	a_{66}^R	Q_{44}	Q_{66}
B1	1.2	2.4	6	6	0.6	1.2	3	3
B2	1.2	2.4	30	30	0.6	1.2	15	15
B3	1.2	2.4	60	60	0.6	1.2	30	30

In all models, the accuracy of the eikonal equation is studied for the direct and transmitted SH waves. The point source is at the origin of coordinates and lies in the upper halfspace. The interface is horizontal at depth $x_3 = -1$ km. The area under study lies in the vertical plane x_1-x_3 , being delimited by x_1 between 0 and 5 km and by x_3 between 0 and -3 km. The travel times are calculated in a grid with steps of 0.01 km in both horizontal and vertical directions.

No overcritical incidences appear in the models used. The overcritical incidences are avoided in the numerical modelling because they can cause difficulties in the complex ray theory in selecting the proper sign of the normal component of the slowness vector at the interface (see Krebes & Daley 2007).

6.2. Complex rays

Since the halfspaces are homogeneous, rays calculated by the complex ray-tracing equations (35) and (36) are straight lines. If the source and receiver lie in the same halfspace, the rays are straight lines in the real space. If the source and receiver lie in different halfspaces, the rays are the piecewise straight lines in the complex space (see Appendix A). The complex rays change their directions at the interface according to the complex Snell's law (complex, real viscoelastic or elastic). The geometry of complex rays is calculated according to Appendix A. The slowness vector of a wave outgoing from the source is generally inhomogeneous. For a direct wave, slowness vector \mathbf{p} is stationary (see Vavryčuk 2007a,b). The energy velocity vector \mathbf{v} and travel time τ are calculated using eqs (A2) and (A3), respectively. For a transmitted wave, the slowness vector \mathbf{p} of the wave outgoing from the source is non-stationary. In Models A, the slowness vector is calculated using eqs (A12) and (A13); in Models B, it is calculated using eqs (A10) and (A11). The complex travel time is calculated using eq. (A9). The point of incidence of a ray at the interface lies in the complex space having a non-zero imaginary coordinate x_1 .

6.3. Real rays

The real-ray approaches are simpler than the complex-ray approach. The real elastic and viscoelastic rays are calculated using eqs (38-39) and (15-16), respectively. The rays are real straight lines in both halfspaces and change their direction at the interface according to the corresponding Snell's law (elastic or viscoelastic). In the elastic-ray approach, all quantities along a real ray are real-valued except for the travel time. The imaginary part of the travel time is calculated using eq. 40. In the viscoelastic-ray approach, the wave quantities along a real ray are generally complex-valued. The complex slowness vector is inhomogeneous, but the complex energy velocity vector is homogeneous. This applies to the direct as well as transmitted wave. The imaginary part of the travel time is calculated by applying the quadrature along the ray (see eq. 17). For a direct wave, the real viscoelastic-ray approach yields an identical solution with the complex-ray approach. For a transmitted wave, the approaches yield different results, the real-ray approach being less accurate.

6.4. Results

The most accurate solution of the complex eikonal equation is obtained using complex ray tracing. The crucial step of the complex ray tracing is to find the point of incidence of a complex ray of the transmitted SH wave at the interface. The start point of a ray is at the source (at the origin of coordinates), and the end point is at the grid of receivers in the lower halfspace. The start and end points lie in the real space, but the point of incidence of a ray at the interface is in complex space.

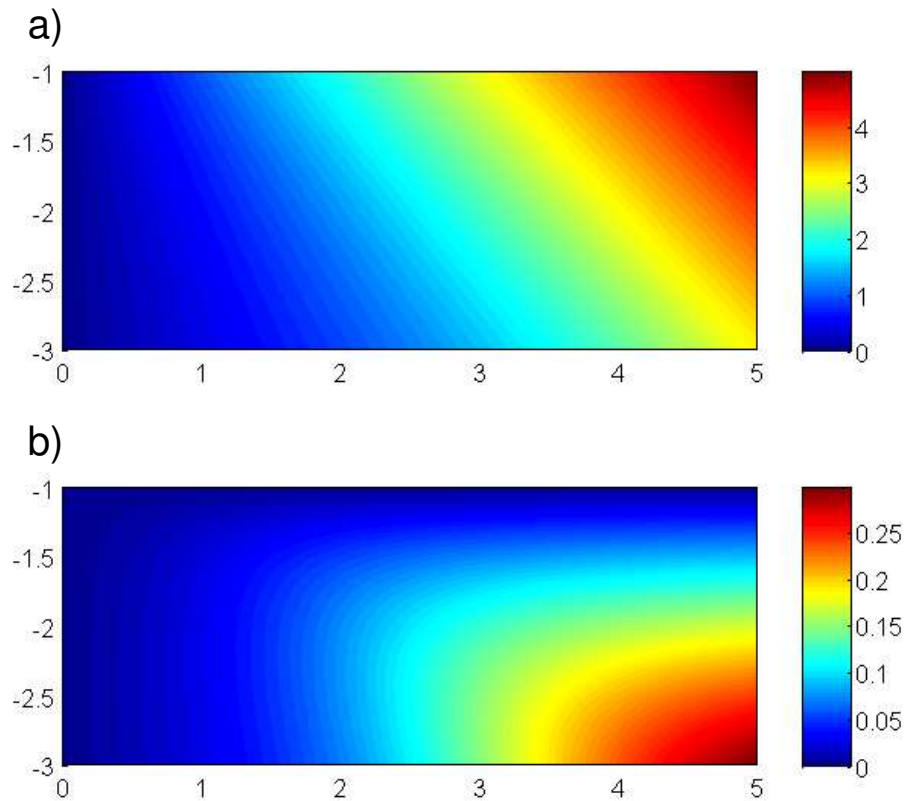


Figure 1. Position of the point of incidence of a complex ray at the interface $x_3 = -1$ for Model A1 as a function of the receiver position in the lower halfspace. The real (a) and imaginary (b) parts of the coordinate x_1 of the incidence point at the interface are shown in colours being the function of the receiver position. The colour scale, and the horizontal and vertical scales are in km.

The positions of the incidence points for the transmitted SH wave in Model A1 are shown in Figure 1. The real and imaginary coordinates of the incidence point vary in dependence on the position of the receiver. For near-vertical incidences the complex rays

do not deviate much from the real plane $x_1^R - x_3^R$. However, for shallower incidences and for greater depths of the receivers, the complex rays can deviate significantly from this plane. Obviously, we can expect that, in this area, the approximate real-ray approaches will reproduce the solution of the eikonal equation with the lowest accuracy.

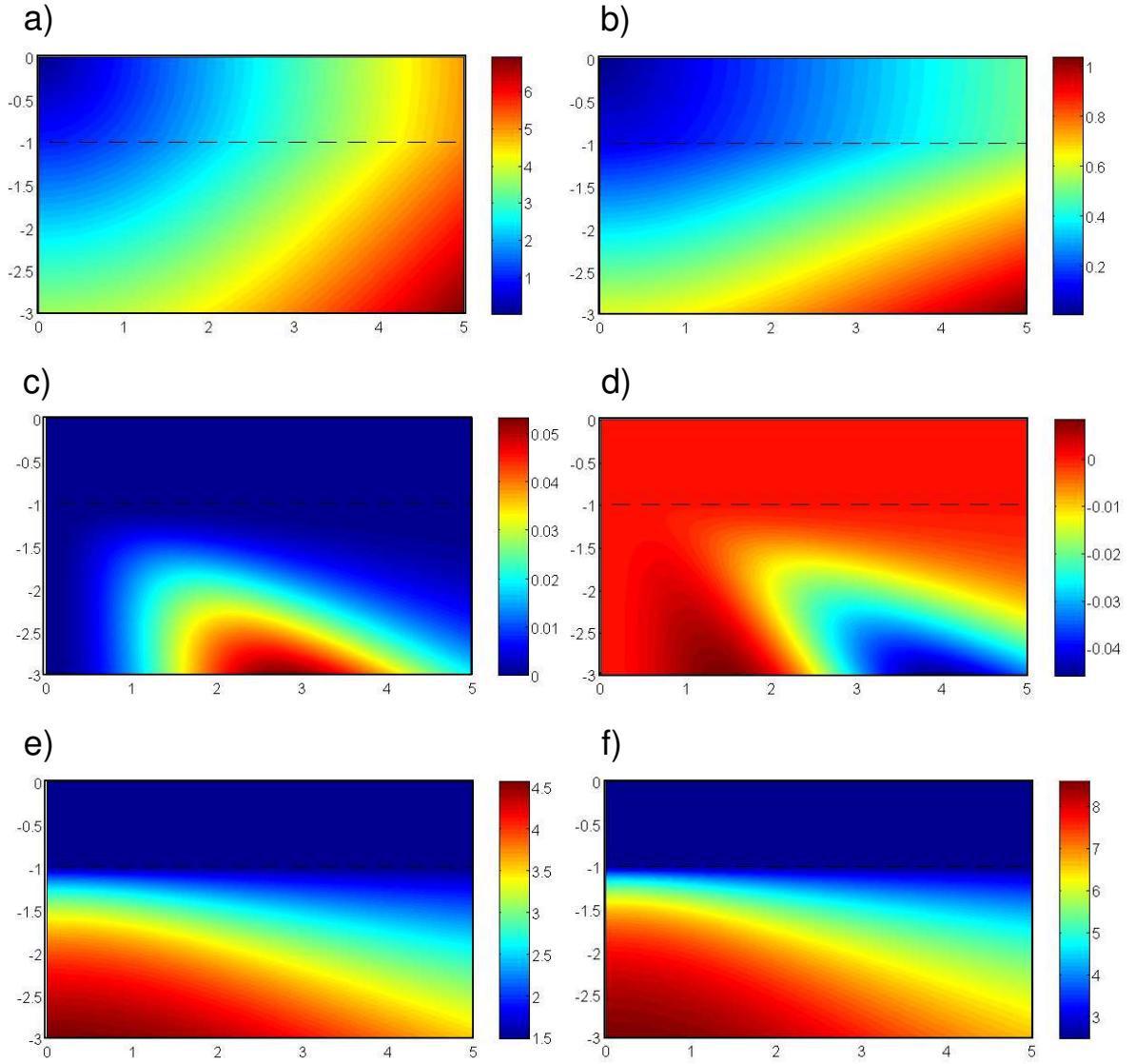


Figure 2. Complex travel time and its errors in Model A1. (a) Real part of the exact travel time, τ^R , (b) imaginary part of the exact travel time, τ^I , (c) errors of τ^R produced by the real viscoelastic ray method, (d) errors of τ^I produced by the real viscoelastic ray method, (e) errors of τ^R produced by the real elastic ray method, (f) errors of τ^I produced by the real elastic ray method. The travel time (a-b) is in seconds, the errors of the travel time (c-f) are in %. The dashed line shows the interface. The horizontal and vertical scales are in km.

Figure 2 shows the exact complex travel time in Model A1 calculated by complex ray tracing (Fig. 2a,b) together with errors produced by real viscoelastic ray tracing (Fig. 2c,d) and by elastic ray tracing (Fig. 2e,f). The errors are calculated at each point of the grid using the following formulas:

$$e_R = \frac{(\tau^{\text{aprox}})^R - (\tau^{\text{exact}})^R}{(\tau^{\text{exact}})^R} 100\% \quad \text{and} \quad e_I = \frac{(\tau^{\text{aprox}})^I - (\tau^{\text{exact}})^I}{(\tau^{\text{exact}})^I} 100\% . \quad (42)$$

The maximum errors e_R and e_I of the complex travel time τ calculated by the real viscoelastic method attain values of up to $5.3 \cdot 10^{-2}\%$ and $4.6 \cdot 10^{-2}\%$, respectively. The real elastic ray method yields errors of up to 4.6% in τ^R and 8.6% in τ^I . Hence, the accuracy of the viscoelastic ray method is about 100 times higher than that of the elastic ray method.

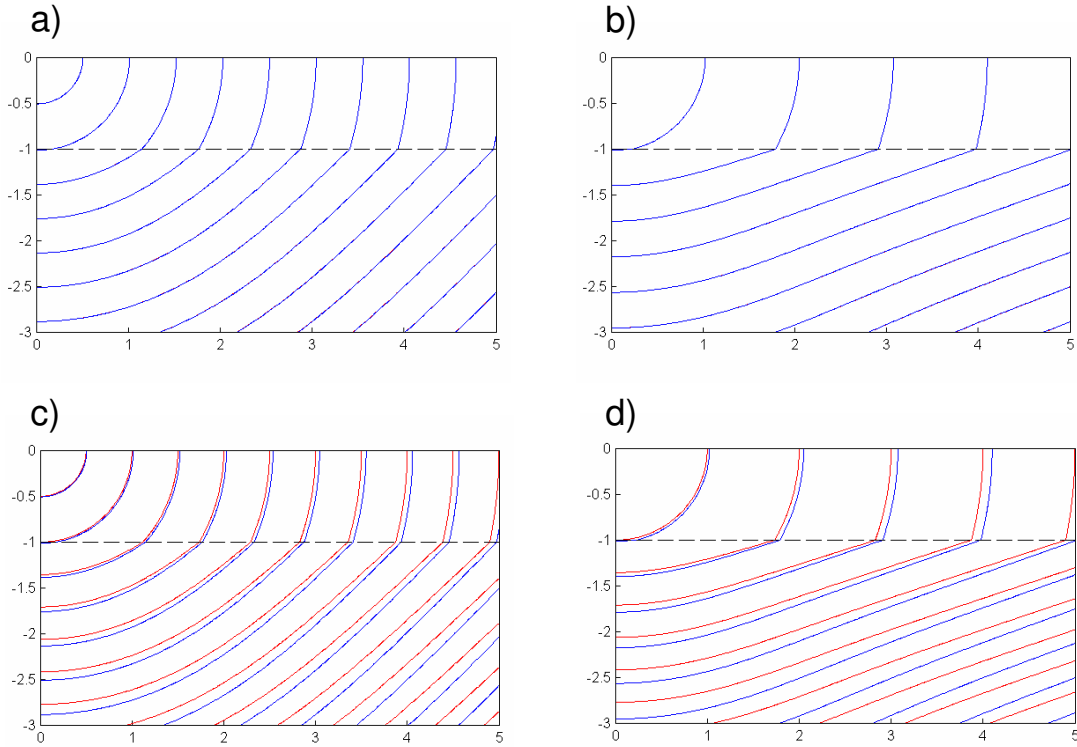


Figure 3. Isochrones in Model A1. Blue line - exact solution calculated using the complex ray theory, red line – approximate solution calculated using the real viscoelastic ray method (a-b), and using the real elastic ray method (c-d). Left-hand plots show the isochrones of the real part of the complex travel time, right-hand plots show the isochrones of the imaginary part of the complex travel time. The steps in the real and imaginary isochrones are 0.5s and 0.1s, respectively. The dashed line shows the interface. The vertical and horizontal scales are in km.

Interestingly, the area of the significant deviation of complex rays from the real plane $x_1^R - x_3^R$ (see Fig. 1) matches the area of low accuracy only very roughly and just for the real viscoelastic rays (see Fig. 2c,d). The errors produced by elastic ray tracing display quite a different pattern: the errors mainly reflect inadequate modelling of the travel time in the extremely attenuating lower halfspace ($Q = 2.5$). This is confirmed in Fig. 3, which shows a comparison of exact and approximate isochrones. The real viscoelastic ray tracing reproduces the isochrones quite well, no remarkable differences between the exact and approximate isochrones are observed (see Fig. 3a,b). However, the real elastic ray tracing produces isochrones deviating from the exact ones. The deviation is particularly visible at greater depths of the lower halfspace (see Fig. 3c,d).

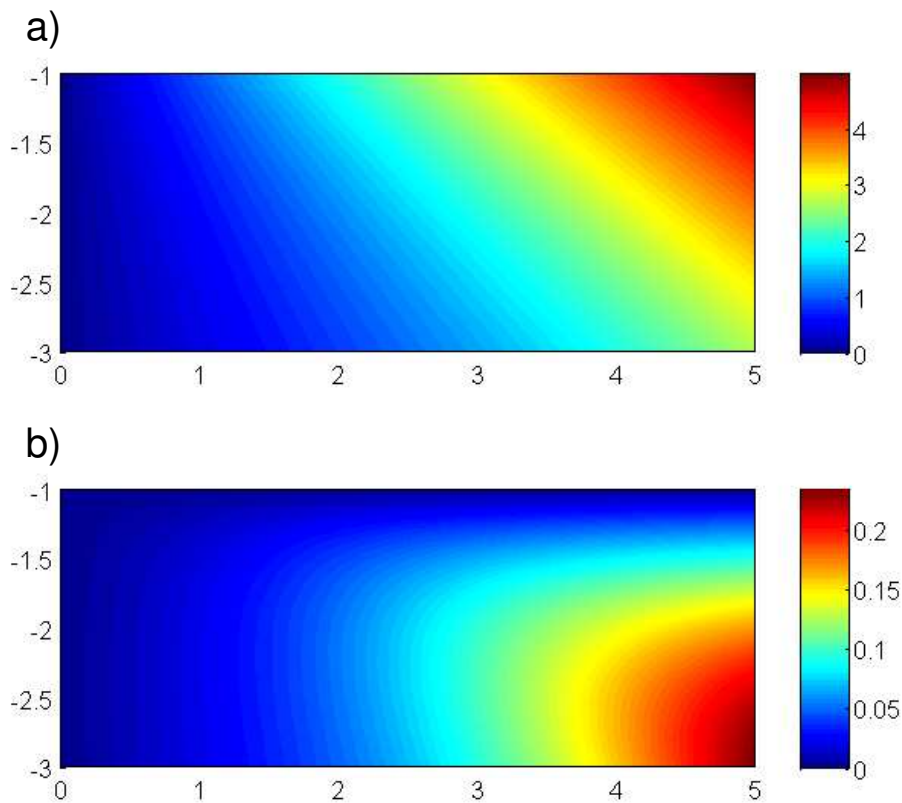


Figure 4. Position of the point of the incidence of a complex ray at the interface $x_3 = -1$ for Model B1 as a function of the receiver position on the lower halfspace. The real (a) and imaginary (b) parts of the coordinate x_1 of the incidence point at the interface are shown in colours being the function of the receiver position. The colour scale, and the horizontal and vertical scales are in km.

Figures 4, 5 and 6 display analogous quantities as Figs 1, 2 and 3, but for Model B1. The results of the numerical modelling for all models are summarized in Tab. 3. The table shows that the real viscoelastic ray tracing is more accurate than the elastic ray tracing in all models. The accuracy is at least 20 times higher for viscoelastic rays than for elastic rays. As expected, in models with low attenuation, the accuracy of both methods increases.

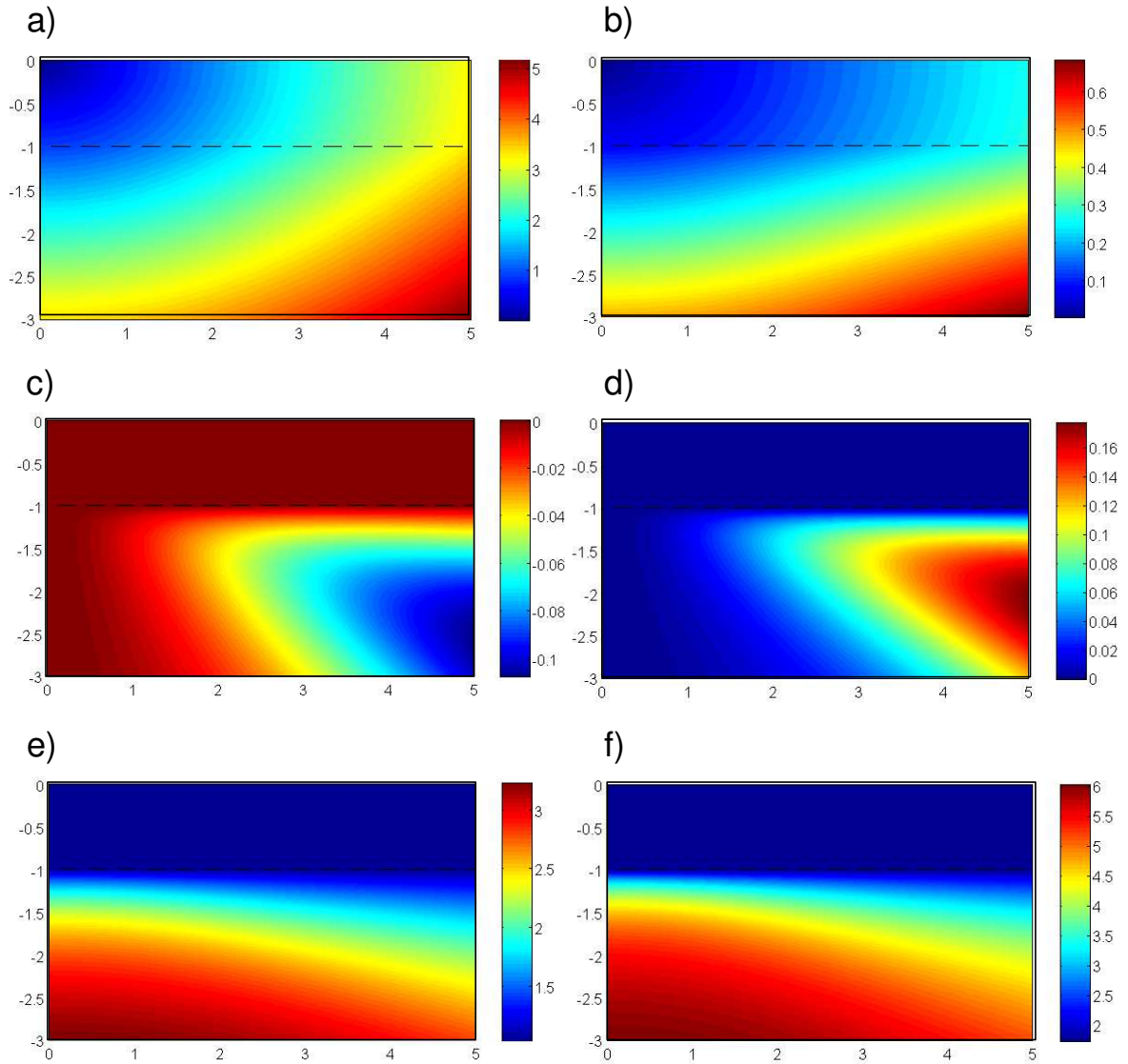


Figure 5. Complex travel time and its errors in Model B1. (a) real part of the exact travel time, τ^R , (b) imaginary part of the exact travel time, τ^I , (c) errors of τ^R produced by the real viscoelastic ray method, (d) errors of τ^I produced by the real viscoelastic ray method, (e) errors of τ^R produced by the real elastic ray method, (f) errors of τ^I produced by the real elastic ray method. The travel time (a-b) is in seconds, the errors of the travel time (c-f) are in %. The dashed line shows the interface. The horizontal and vertical scales are in km.

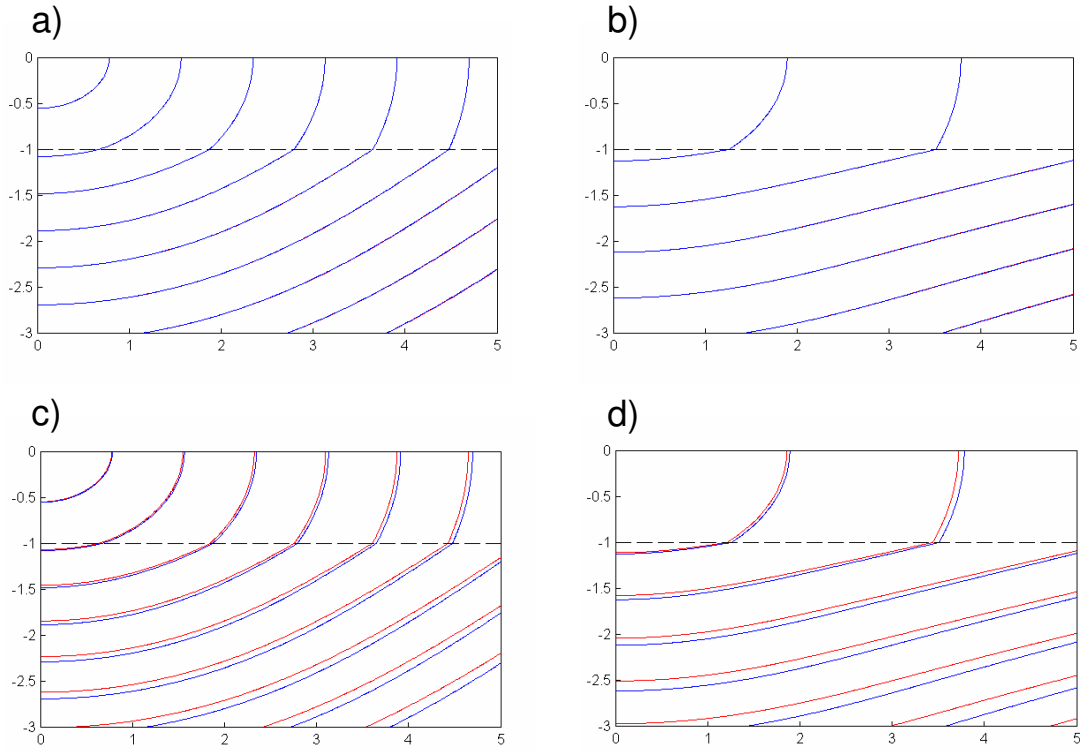


Figure 6. Isochrones in Model B1. Blue line - exact solution calculated using the complex ray theory, red line – approximate solution calculated using the real viscoelastic ray method (a-b), and using the real elastic ray method (c-d). Left-hand plots show the isochrones of the real part of the complex travel time, right-hand plots show the isochrones of the imaginary part of the complex travel time. The steps in the real and imaginary isochrones are 0.5s and 0.1s, respectively. The dashed line shows the interface. The vertical and horizontal scales are in km.

Table 3: Errors in the complex travel time produced by real ray methods

Model	Elastic rays		Viscoelastic rays	
	e^R (%)	e^I (%)	e^R (%)	e^I (%)
A1	4.6	8.6	$5.3 \cdot 10^{-2}$	$4.6 \cdot 10^{-2}$
A2	$1.9 \cdot 10^{-1}$	$3.5 \cdot 10^{-1}$	$2.2 \cdot 10^{-3}$	$2.2 \cdot 10^{-3}$
A3	$4.8 \cdot 10^{-2}$	$8.9 \cdot 10^{-2}$	$5.6 \cdot 10^{-4}$	$5.6 \cdot 10^{-4}$
B1	3.2	6.0	$1.1 \cdot 10^{-1}$	$1.8 \cdot 10^{-1}$
B2	$1.3 \cdot 10^{-1}$	$2.5 \cdot 10^{-1}$	$4.6 \cdot 10^{-3}$	$7.4 \cdot 10^{-3}$
B3	$3.4 \cdot 10^{-2}$	$6.2 \cdot 10^{-2}$	$1.1 \cdot 10^{-3}$	$1.9 \cdot 10^{-3}$

7. DISCUSSION

The most accurate approach for calculating rays in anisotropic viscoelastic media is the complex ray theory. The rays are calculated using complex ray-tracing equations in smoothly inhomogeneous media and obey the complex Snell's law at the interface. The complex Snell's law constrains complex tangential components of slowness vector \mathbf{p} . The normal components are calculated using the Christoffel equation. The start and end points of a complex ray lie in the real space, but the point of incidence at the interface lies in the complex space.

Less accurate but computationally more efficient approaches are the real viscoelastic and elastic ray methods. The ray tracing equations are simpler and produce real rays. At the interface, the rays obey the real viscoelastic or elastic Snell's law, respectively. The real Snell's laws bind the tangential components of the real part of slowness vectors \mathbf{p}_Σ^R . All wave quantities along a real ray in the elastic ray approach are real-valued except for the travel time. The imaginary part of the travel time is calculated by applying the quadrature along the ray. In the viscoelastic ray approach, the wave quantities along a ray are complex-valued. The complex-valued slowness vector must be stationary. Similarly as in the elastic ray approach, the imaginary part of the travel time is calculated by applying the quadrature along a ray.

Applying the real viscoelastic Snell's law is more involved than applying the elastic Snell's law. In the elastic ray theory, the slowness vector is real-valued. The elastic Snell's law constrains its tangential components \mathbf{p}_Σ^R , and the normal components \mathbf{p}_n^R are calculated using the Christoffel equation. The sign of \mathbf{p}_n^R is selected according to the proper ray direction and the radiation conditions. In the viscoelastic ray theory, the slowness vector is complex-valued. The viscoelastic Snell's law constrains the real parts of the tangential components \mathbf{p}_Σ^R , but not the imaginary parts \mathbf{p}_Σ^I . Therefore, in order to determine the complete slowness vector of scattered waves, the other missing components: \mathbf{p}_n^R , \mathbf{p}_Σ^I and \mathbf{p}_n^I , must be calculated. The components \mathbf{p}_n^R and \mathbf{p}_n^I are calculated using the Christoffel equation, the component \mathbf{p}_Σ^I can be found using the condition of the stationarity of the slowness vector. However, this computation cannot be done at one step, but by iterations. At this point, the procedure is different from that applied to the complex ray theory. In calculating the complex slowness vector by applying the complex Snell's law, the tangential components of the complete slowness vector \mathbf{p}_Σ are conserved. This condition is stronger than that required by the real viscoelastic Snell's law. Consequently, normal component \mathbf{p}_n can be calculated more easily in the complex ray approach, and no procedure with iterations is needed. In isotropic media, the real viscoelastic ray approach simplifies.

Since the slowness vector is homogeneous for all scattered waves, no iterations are needed in calculating the missing components of \mathbf{p} : \mathbf{p}_n^R , \mathbf{p}_Σ^I and \mathbf{p}_n^I .

Numerical modelling shows that the real viscoelastic ray approach is highly accurate. Isotropic and anisotropic models with various levels of attenuation ranging from extremely strong ($Q = 2.5-3$) to moderate attenuation ($Q = 25-30$) have been used to demonstrate that the real viscoelastic approach is at least 20 times more accurate than the real elastic ray approach. In isotropic media, the computational requirements are essentially the same for both methods. In anisotropic media, the viscoelastic ray approach is more computationally demanding.

ACKNOWLEDGEMENTS

The work was supported by the Grant Agency of the Academy of Sciences of the Czech Republic, Grant No. IAA300120801, and by the Consortium Project “Seismic Waves in Complex 3-D Structures”.

REFERENCES

- Amodei, D., Keers, H., Vasco, W. & Johnson, L., 2006. Computation of uniform wave forms using complex rays, *Physical Review E*, **73**, 036704, 1-14.
- Borcherdt R.D., 1977. Reflection and refraction of type-II S waves in elastic and anelastic media. *Bull. Seism. Soc. Am.*, **67**, 43-67.
- Borcherdt R.D., 1982. Reflection-refraction of general P- and type-I S waves in elastic and anelastic solids. *Geophys. J. R. Astr. Soc.*, **70**, 621-638.
- Carcione, J.M., 1990. Wave propagation in anisotropic linear viscoelastic media: theory and simulated wavefields, *Geophys. J. Int.*, **101**, 739-750. Erratum: 1992, **111**, 191.
- Carcione, J.M., 1993. Seismic modelling in viscoelastic media, *Geophysics*, **58**, 110-120.
- Carcione, J.M., 2006. Vector attenuation: elliptical polarization, raypaths and the Rayleigh-window effect, *Geophys. Prospecting*, **54**, 399-407.
- Carcione, J.M., 2007. *Wave Fields in Real Media. Theory and Numerical Simulation of Wave Propagation in Anisotropic, Anelastic, Porous and Electromagnetic Media*, Elsevier.
- Caviglia, G. & Morro, A., 1992. *Inhomogeneous Waves in Solids and Fluids*, World Scientific, London.
- Červený, V., 2001. *Seismic Ray Theory*, Cambridge University Press, Cambridge, U.K.
- Červený, V., 2007. Reflection/transmission laws for slowness vectors in viscoelastic anisotropic media, *Stud. Geophys. Geod.*, **51**, 391-410.

- Červený, V., & Pšenčík, I., 2005. Plane waves in viscoelastic anisotropic media – I. Theory, *Geophys. J. Int.*, **161**, 197-212.
- Červený, V., Klimeš, L. & Pšenčík, I., 2008. Attenuation vector in heterogeneous, weakly dissipative, anisotropic media, *Geophys. J. Int.*, **175**, 346-355.
- Chapman, S.J., Lawry, J.M.H., Ockendon, J.R. & Tew, R.H., 1999. On the theory of complex rays, *SIAM Review*, **41**, 417-509.
- Gajewski, D. & Pšenčík, I., 1992. Vector wavefield for weakly attenuating anisotropic media by the ray method, *Geophysics*, **57**, 27-38.
- Hanyga, A., & Sereďyňska, M., 2000. Ray tracing in elastic and viscoelastic media, *Pure Appl. Geophys.*, **157**, 679-717.
- Hearn, D. J., & Krebes, E. S., 1990a. On computing ray-synthetic seismograms for anelastic media using complex rays, *Geophysics*, **55**, 422-432.
- Hearn, D. J., & Krebes, E. S., 1990b. Complex rays applied to wave propagation in a viscoelastic medium, *Pure Appl. Geophys.*, **132**, 401-415.
- Klimeš, L., 2002. Second-order and higher-order perturbations of travel time in isotropic and anisotropic media, *Stud. Geophys. Geod.*, **46**, 213-248.
- Kravtsov, Yu.A., 2005. *Geometrical Optics in Engineering Physics*, Alpha Science, Harrow, U.K.
- Kravtsov, Yu.A., Forbes, G.W. & Asatryan, A.A., 1999. Theory and applications of complex rays, in *Progress in Optics*, ed. E. Wolf (Amsterdam, Elsevier 1999), vol. **39**, pp. 3-62.
- Krebes E.S. and Daley P.F., 2007. Difficulties with computing anelastic plane wave reflection and transmission coefficients. *Geophys. J. Int.*, **170**, 205-216 doi: 10.1111/j.1365-246X.2006.03349.x.
- Le, L.H.T., Krebes, E.S., Quiroga-Goode, G.E., 1994. Synthetic seismograms for *SH* waves in anelastic transversely isotropic media, *Geophys. J. Int.*, **116**, 598-604.
- Moczo, P., Kristek, J. & Halada, L., 2004. *The Finite-Difference Method for Seismologists. An Introduction*. Comenius University, Bratislava. 158 pp., ISBN 80-223-2000-5.
- Moczo, P., Kristek, J., Gális, M., Pažák, P. & Balazovjeh, M., 2007. The finite-difference and finite-element modeling of seismic wave propagation and earthquake motion, *Acta Physica Slovaca*, **57**(2), 177-406.
- Thomson, C.J., 1997. Complex rays and wave packets for decaying signals in inhomogeneous, anisotropic and anelastic media, *Stud. Geophys. Geod.*, **41**, 345-381.
- Saenger, E.H. & T. Bohlen, 2004. Finite-difference modeling of viscoelastic and anisotropic wave propagation using the rotated staggered grid, *Geophysics*, **69**, 583-591, doi:10.1190/1.1707078.

- Vavryčuk, V., 2007a. Asymptotic Green's function in homogeneous anisotropic viscoelastic media, *Proc. Roy. Soc.*, A **463**, 2689-2707, doi:10.1098/rspa.2007.1862.
- Vavryčuk, V., 2007b. Ray velocity and ray attenuation in homogeneous anisotropic viscoelastic media, *Geophysics*, No. 6, **72**, D119-D127, doi:10.1190/1.2768402.
- Vavryčuk, V., 2008a. Real ray tracing in anisotropic viscoelastic media, *Geophys. J. Int.*, **175**, 617-626, doi: 10.1111/j.1365-246X.2008.03898.x.
- Vavryčuk, V., 2008b. Velocity, attenuation and quality factor in anisotropic viscoelastic media: a perturbation approach, *Geophysics*, **73**, No. 5, D63-D73, doi: 10.1190/1.2921778.
- Vavryčuk, V., 2009. Accuracy of real ray tracing in isotropic viscoelastic media, *Geophys. J. Int.*, submitted.
- Wennerberg, L., 1985. Snell's law for viscoelastic materials, *Geophys. J. Roy. Astr. Soc.*, **81**, 13-18.
- Winterstein, D.F., 1987. Vector attenuation: Some implications for plane waves in anelastic layered media, *Geophysics*, No. 6, **52**, 810-814.

APPENDIX A: COMPLEX RAY TRACING IN A MEDIUM WITH TWO HOMOGENEOUS HALFSPACES

Let us assume two homogeneous viscoelastic halfspaces separated by a plane horizontal interface at $x_3 = 0$. The source is situated in the upper halfspace and the receiver in the lower halfspace. Both source and receiver lie in the x - z plane. The homogeneous halfspaces defined in the real space are analytically continued to be homogeneous in the complex space. The interface in the complex space is defined by $x_3 = x_3^R + ix_3^I = 0$.

The solution of the complex ray-tracing equations (35-36) is elementary in both halfspaces and yields

$$x_i = v_i \tau, \quad (\text{A1})$$

where energy velocity vector \mathbf{v} ,

$$v_i = a_{ijkl} g_j g_k p_l, \quad (\text{A2})$$

and slowness vector \mathbf{p} are constant along the complex ray. If the source and receiver lie in the same halfspace, the ray defined as $\mathbf{x} = \mathbf{x}(\tau)$ is a straight line in real space. The complex

energy velocity vector \mathbf{v} is homogeneous and slowness vector \mathbf{p} is stationary. The stationary slowness vector \mathbf{p} can be calculated using the procedure described in Vavryčuk (2007a,b). The complex travel time τ is expressed as

$$\tau = \mathbf{p} \cdot \mathbf{x}, \quad (\text{A3})$$

and its real and imaginary parts are related by the following equation:

$$\tau^I = -\frac{v^I}{v^R} \tau^R. \quad (\text{A4})$$

If the source and receiver lie in different halfspaces, the ray consists of two straight line segments. Both segments are, in general, in complex space, only the start and end points of the ray lie in real space. If we denote the ray segments in the upper and lower halfspaces by superscripts A and B , respectively,

$$x_1 = x_1^A + x_1^B, \quad x_3^A = \frac{v_1^A}{v_3^A} x_3^A, \quad x_3^B = \frac{v_1^B}{v_3^B} x_3^B. \quad (\text{A5})$$

Taking into account that

$$\tan i^A = \frac{v_1^A}{v_3^A}, \quad \tan i^B = \frac{v_1^B}{v_3^B}, \quad (\text{A6})$$

we obtain

$$x_1 - x_3^A \tan i^A - x_3^B \tan i^B = 0, \quad (\text{A7})$$

where x_1 is the horizontal distance between the source and the receiver, i^A and i^B are angles of a ray at the source and receiver, respectively. Coordinates x_1 , x_3^A and x_3^B are real, angles i^A and i^B are complex. The ray angles i^A and i^B are functions of slowness vectors \mathbf{p}^A and \mathbf{p}^B at the source and at the receiver and can be calculated by applying eqs (35) and (A6). The horizontal component of slowness vector \mathbf{p}^B is obtained from \mathbf{p}^A by applying the complex Snell's law at the interface:

$$p_1^A = p_1^B. \quad (\text{A8})$$

The vertical component of \mathbf{p}^B is obtained using the Christoffel equation (see Section 4.2). Hence, eq. (A7) is actually the equation for the unknown complex take-off angle i_p^A of slowness vector \mathbf{p}^A . Having calculated angle i_p^A , and consequently slowness vectors \mathbf{p}^A and \mathbf{p}^B , the travel time comes out as

$$\tau = \tau^A + \tau^B = p_1^A x_1 + p_3^A x_3^A + p_3^B x_3^B . \quad (\text{A9})$$

In transversely isotropic media, eq. (A7) simplifies for the SH wave to

$$x_1 - x_3^A \frac{a_{66}^A}{a_{44}^A} \tan i_p^A - x_3^B \frac{a_{66}^B}{a_{44}^B} \tan i_p^B = 0 , \quad (\text{A10})$$

where

$$\tan i_p^A = \frac{p_1^A}{p_3^A}, \quad \tan i_p^B = \frac{p_1^B}{p_3^B} = \frac{p_1^A}{p_3^B} . \quad (\text{A11})$$

In isotropic media, eq. (A7) yields for the P or S waves

$$x_1 - x_3^A \tan i_p^A - x_3^B \tan i_p^B = 0 , \quad (\text{A12})$$

where

$$\tan i_p^A = \frac{p_1^A}{\sqrt{(c^A)^{-2} - (p_1^A)^2}}, \quad \tan i_p^B = \frac{p_1^A}{\sqrt{(c^B)^{-2} - (p_1^A)^2}} . \quad (\text{A13})$$

Quantities c^A and c^B are the complex phase velocities in the upper and lower halfspaces, respectively.